Almedina Modrić-Šahbazović[1,], Zerina Sakić[1], Maja Đekić[2]*

[1]University of Tuzla, Faculty of Natural Sciences and Mathematics, Tuzla, Bosnia and Herzegovina, [2]University of Sarajevo, Faculty of Science, Sarajevo, Bosnia and Herzegovina

Scientific paper
ISSN 0351-9465, E-ISSN 2466-2585
https://doi.org/10.62638/ZasMat1760

Zastita Materijala 67 ()
(2026)

Tuning microstructural and optical properties of ZnO thin films on p-type Si(100)

ABSTRACT

Very thin ZnO films were fabricated on p-type Si (100) substrates using two different solvents, methanol (M) and 2-methoxyethanol (2M), via a simple spin-coating method. Five-layer ZnO films were characterized structurally using X-ray diffraction (XRD), with detailed analysis performed using the Williamson–Hall (W-H) method. Surface morphology was examined by scanning electron microscopy (SEM) and atomic force microscopy (AFM), while ultraviolet–visible (UV–Vis) spectroscopy provided optical properties, including the optical band gap determined via the Kubelka–Munk theory. The crystallite sizes calculated from W-H models were larger than those estimated by the Debye–Scherrer method, indicating that peak broadening is influenced by both crystallite size and lattice strain. Strain, stress, and deformation energy density values, derived from the Uniform Deformation Model (UDM), Uniform Stress Deformation Model (USDM), and Uniform Deformation Energy Density Model (UDEDM), respectively, were higher in films prepared with 2-methoxyethanol than methanol. ZnO films from 2-methoxyethanol exhibited greater homogeneity and lower surface roughness, while their optical band gap (~3.3 eV) was slightly higher than that of methanol-derived films (~3.02 eV) but still below bulk ZnO (3.37 eV). These results show that ZnO thin films prepared with 2-methoxyethanol exhibit superior microstructural, mechanical, and optical properties, producing smoother and more uniform films with enhanced optical characteristics, and are therefore more commonly preferred for optoelectronic and photovoltaic applications due to their improved crystallinity, low surface roughness, and suitable band gap.

Keywords: *ZnO, thin film, sol-gel, spin-coater, solvent*

1. INTRODUCTION

In recent years, research in the field of nanotechnology has experienced rapid development and has attracted the interest of a large number of scientists [1]. Thin films exhibit specific properties thatare different from those of bulk materials [2]. One area of significant interest is metal oxide semiconductors due to their tunable optical, electronic, magnetic, and catalytic properties, with zinc oxide being particularly prominent among them [3–8]. Its non-toxicity, photochemical properties, and chemical stability make it an excellent candidate for photocatalytic applications, antibacterial applications, and drug delivery systems [9–11]. In addition to these applications, ZnO thin films are also used as functional layers in solar cells, gas and pH sensors, varistors, and related devices [12–16].

*Corresponding author:Almedina Modrić-Šahbazović
E-mail: almedina.modricsahbazovic@untz.ba
Paper received: 04.02.2026.
Paper corrected: 24.02.2026.
Paper accepted: 03.03.2026.

It is well known that a wide variety of methods are available for thin-film fabrication, such as Physical Vapor Deposition (PVD), Pulsed Laser Deposition (PLD), DC plasma sputtering, Molecular Beam Epitaxy (MBE), Chemical Vapor Deposition (CVD), Atomic Layer Deposition (ALD), the sol–gel method, spin coating, dip coating, and others [17–22]. Among these, the sol–gel method combined with spin coating has proven to be one of the most efficient and fastest approaches for producing a large number of homogeneous ZnO thin films [23–27]. This technique can be carried out at relatively low temperatures, reducing the risk of thermal damage to the substrate while ensuring high film reproducibility.

For these reasons, the sol–gel spin-coating method was used in this study as a highly efficient, fast, simple, and cost-effective approach for the fabrication of uniform ZnO thin films on p-type Si (100) substrates. Although zinc oxide (ZnO) thin films have been extensively investigated due to their attractive properties, many questions remain unanswered regarding the relationship between fabrication conditions and the resulting morphology

and optical characteristics of the material. These include the choice of solvent, temperature, reaction time, precursor concentration, substrate selection, spin speed and duration, as well as post-annealing temperature. The main objective of this work was to investigate the influence of the solvent on the final properties of ZnO thin films. For this purpose, XRD, SEM, AFM, and UV–Vis techniques were employed, providing a significant contribution to their potential functional applications.

2. EXPERIMENTAL

ZnO thin films were fabricated using a spin coater (Model P-6708D, Specialty Coating Systems, Indianapolis, IN, USA) capable of reaching a maximum rotation speed of 8000 rpm. The deposition process requires a precursor solution to be applied onto an appropriate substrate. The solution was prepared by a sol–gel synthesis route, in which zinc acetate was dissolved in an organic solvent (methanol or 2-methoxyethanol) for 30 min at 60 °C with the addition of a stabilizer (ethanolamine), followed by further stirring for 90 min at 60 °C. Based on preliminary investigations, the optimal zinc acetate concentration was selected as 0.2 M, and the ideal molar ratio of stabilizer to zinc was chosen to be 1:1.

After aging for several days, the resulting solutions were deposited onto p-type Si (100) substrates using the spin coater. Prior to deposition, the substrates were cleaned in an ultrasonic bath for 10 min each in distilled water, acetone, and ethanol, and then dried in an air stream. To obtain homogeneous ZnO thin films, the rotation speed and spinning time were optimized; in this study, values of 2000 rpm and 40 s were used. After the deposition of each layer, the films were heated at 160 °C for 10 min to ensure complete evaporation of the solvent. This procedure was repeated several times to obtain five-layer ZnO thin films, which were subsequently thermally annealed at 500 °C for 1 h.

The crystalline structure of the obtained ZnO thin films was determined using a Bruker D8 Advance X-ray diffractometerwith CuKα radiation beam (wavelenght, λ = 0.154 nm) incident on the sample at a small angle. The morphology of the ZnO thin films was analyzed using a FEI Scios2 Dual Beam scanning electron microscope, which was also used to obtain cross-sectional images of selected samples. Information on the surface topography of the ZnO nanofilms was obtained using an atomic force microscope (AFM, Nanosurf CoreAFM) with a resolution of 1 nm. The UV–visible spectra were recorded using a PerkinElmer Lambda 365 UV–Vis spectrophotometer in the wavelength range of 190–1100 nm with a spectral resolution of 0.5 nm.

3. RESULTS AND DISCUSSIONS

3.1. Microstructural properties

The structural properties of ZnO thin films prepared from solutions with different solvents (methanol and 2-methoxyethanol) on p-type silicon substrates were characterized by X-ray diffraction (XRD), and the obtained XRD patterns are shown in Fig. 1a.

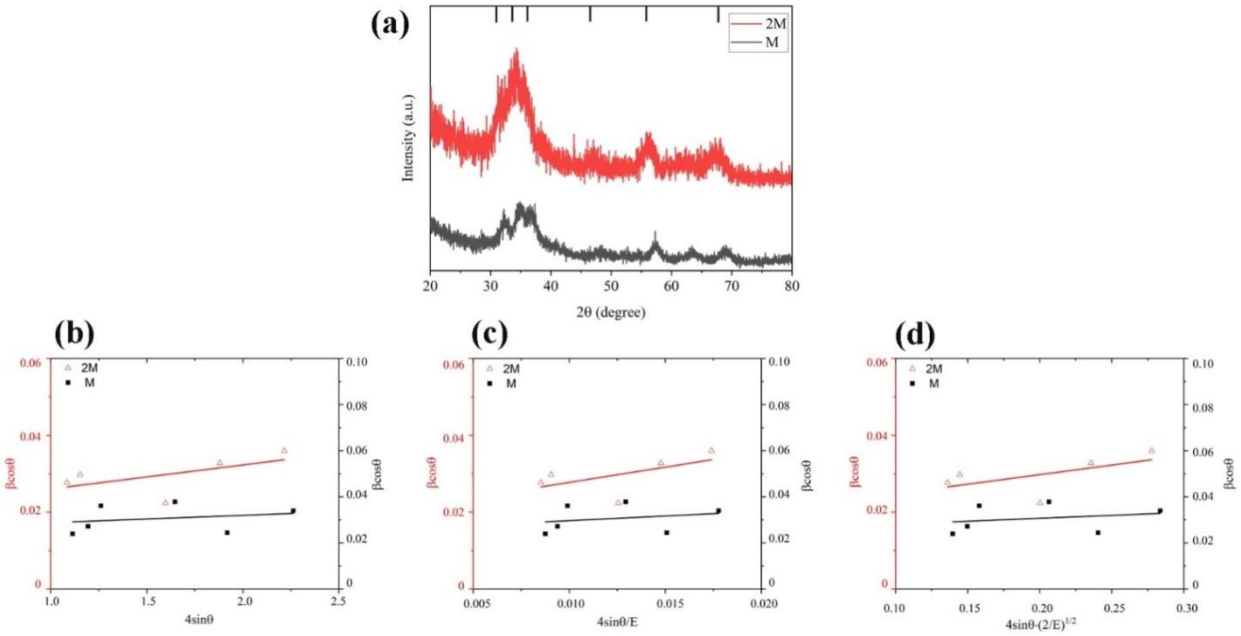

Figure 1. X-ray diffraction (XRD) patterns of ZnO thin films prepared using various solvents (a), Williamson–Hall analysis based on the Uniform Deformation Model (UDM) (b), and modified Williamson–Hall models: the Uniform Stress Deformation Model (USDM) (c) and the Uniform Deformation Energy Density Model (UDEDM) (d)

The obtained diffractograms confirm the hexagonal wurtzite structure of ZnO, as the characteristic diffraction peaks of the ZnO thin films prepared using methanol and 2-methoxyethanol correspond to the (100), (002), (101), (102), (110), and (112) planes and are in very good agreement with the standard ICDD card No. 0036–1451.

The positions of these reflections are clearly indicated by vertical lines in the diffractogram. Specifically, the methanol-based sample exhibits peaks at 2θ = 32.34937°, 34.76045°, 36.76217°, 48.64421°, 57.35853°, and 68.92783°, while the 2-methoxyethanol sample shows peaks at 31.48431°, 33.51930°, 34.85109°, 47.09616°, 56.09323°, and 67.31621°.The peak intensities are slightly higher for ZnO thin films prepared using 2-methoxyethanol, indicating a higher degree of crystallinity. In both cases, a hexagonal wurtzite crystal structure was confirmed.

A perfect crystal, with a completely regular atomic arrangement and infinite periodicity, represents an ideal that cannot be achieved in practice. Real crystals have a finite size and various defects, which lead to broadening of diffraction peaks and enable the estimation of crystallite size. In this context, the crystallite size often differs from the particle size, since many particles are polycrystalline and consist of several smaller crystallites.The average crystallite size of the ZnO thin films was calculated using the Debye–Scherrer formula [28]:

$$D = \frac{0.9 \cdot \lambda}{\beta \cdot \cos\theta} \qquad (1)$$

where: D is the crystallite size, k = 0.9 is the shape factor for spherical crystallites, λ is the X-ray wavelength (CuKα = 0.15406 nm), θ is the Bragg angle of the most intense peak, and β is the full width at half maximum (FWHM) of the peak.After calculation, it was found that the crystallite size of the thin films prepared using 2-methoxyethanol is 4.34 nm, while that of the films prepared using methanol is slightly larger, measuring 4.69 nm.

The Debye–Scherrer equation considers only the broadening of XRD peaks due to crystallite size, neglecting lattice microstructure effects such as strain, which can arise from point defects, grain boundaries, dislocations, and stacking faults [29]. To overcome this limitation, methods such as the Williamson–Hall (W–H) analysis have been developed, which is considered a simple and accurate method for estimating geometric parameters such as microstrain, stress, and deformation energy density. This includes models such as the Uniform Deformation Model (UDM), the Uniform Stress Deformation Model (USDM), and the Uniform Deformation Energy Density Model (UDEDM).

Assuming the crystal is isotropic, the UDM accounts for uniform strain along all crystallographyc directions. Thus, the broadening of a given diffraction peak (β) is influenced not only by crystallite size but also by this uniform strain, which can be expressed by the relation:

$$\beta \cdot \cos\theta = \frac{k \cdot \lambda}{D} + 4 \cdot \varepsilon \cdot \sin\theta \qquad (2)$$

where ε is the strain.

The isotropic strain ε in the UDM can be estimated from the slope of the plot of $\beta \cos\theta$ as a function of $4 \sin\theta$, while the average crystallite size can be determined from the intersection of the linear fit with the vertical axis, i.e., from the Williamson–Hall plot (Fig. 1b). From the figure, it is evident that the slope is positive for both solvents, indicating the presence of relative broadening. As a result, the crystallite size increases compared to the values calculated using the Debye–Scherrer model, with the obtained values being 7 nm for the 2-methoxyethanol solvent and 6.87 nm for methanol.

While UDM is widely used, in many cases, the assumption of homogeneity and isotropy is not satisfied, and an anisotropic approach is adopted, namely the Uniform Stress Deformation Model (USDM), assuming that (an anisotropic strain exists in the crystal) small microstrains are present in the particles. In the USDM, Hooke's law is applied to stress, establishing a linear proportionality between stress and strain as given by:

$$\sigma = \varepsilon \cdot E \qquad (3)$$

where σ is the crystal stress, ε is the anisotropic microstrain that depends on the crystallographic directions, and E is Young's modulus, which for ZnO with a hexagonal structure has a value of approximately 127 GPa. In this approach, by substitution, the Williamson–Hall equation becomes

$$\beta \cdot \cos\theta = \frac{k \cdot \lambda}{D} + 4 \cdot \frac{\sigma}{E} \cdot \sin\theta \qquad (4)$$

This equation is only an approximation and is valid for relatively small stresses (when the stress increases, the particles deviate from this linear proportionality). By plotting $\beta \cos\theta$ as a function of $4 \sin\theta / E$ (Fig. 1c), the stress σ can be determined

from the slope, while the y-intercept gives the crystallite size. The strain ε can be calculated if Young's modulus E is known (Table 1).

Table 1. Crystallite sizes from Debye–Scherrer and Williamson–Hall methods, along with strain, stress, and deformation energy density of ZnO thin films prepared with methanol and 2-methoxyethanol

Sample	Scherrer's method	Williamson-Hall method			
	D (nm)	D (nm)	$\varepsilon \cdot 10^{-3}$	σ (MPa)	u (KJm^{-3})
M	4.69	5.41	3.17	402.59	638.10
2M	4.34	7.00	6.24	792.48	2472.54

There is another model called the Uniform Deformation Energy Density Model (UDEDM), which can be used to determine the deformation energy density of the crystal. Since the assumption of homogeneity and isotropy is not justified, the proportionality constants related to the stress–strain relationship are no longer independent when the deformation energy density u is considered. For an elastic system following Hooke's law, the energy density u (energy per unit volume) as a function of strain is given by $u = (\varepsilon^2 E)/2$. Accordingly, the Williamson–Hall equation takes the form:

$$\beta \cdot \cos\theta = \frac{k \cdot \lambda}{D} + 4 \cdot \left(\frac{2u}{E}\right)^{1/2} \cdot \sin\theta \qquad (5)$$

The plot of $\beta \cos\theta$ as a function of $4 \sin\theta \cdot (2/E)^{1/2}$ is shown in Fig. 1d, where the anisotropic deformation energy density u is estimated from the slope, and the crystallite size is determined from the y-intercept (Table 1).

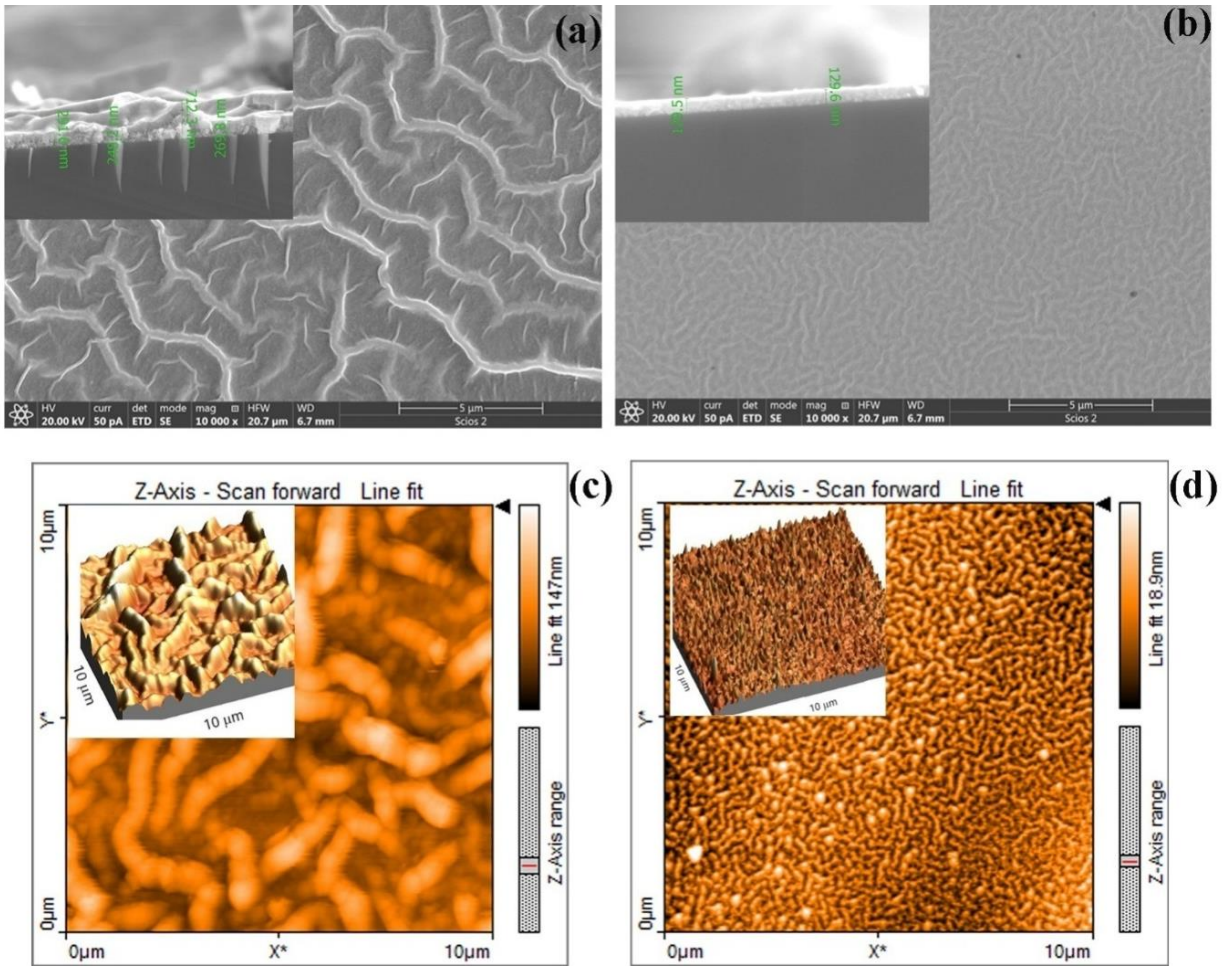

Figure 2. SEM micrographs of ZnO thin films prepared using methanol (a) and 2-methoxyethanol (b), with cross-sectional images shown in the insets, and AFM images of the films prepared with methanol (c) and 2-methoxyethanol (d), with corresponding 3D surface images shown in the insets

The morphological characteristics of ZnO thin films were examined using a scanning electron microscope (SEM). FESEM micrographs of ZnO thin films on p-type silicon substrates prepared with methanol as the solvent are shown in Fig. 2a, while films prepared with 2-methoxyethanol are shown in Fig. 2b. The insets in Figs. 2a and 2b show cross-sectional SEM images of the films, clearly distinguishing the film and substrate regions. The ZnO thin film prepared from methanol (Fig. 2a) is considerably thicker, with measured values ranging from approximately 248.2 nm to 712.3 nm, reflecting pronounced structural inhomogeneity. Surface wrinkling is observed, which can be attributed to the low boiling point of methanol (≈64.7 °C) causing rapid solvent evaporation during drying. This rapid removal induces localized mechanical stresses in the surface layer, leading to the formation of pronounced wrinkles. Additionally, the increase in substrate temperature during drying further accelerates solvent evaporation, generating stress between the film and substrate, which prevents a reliable determination of a representative thickness. In contrast, the ZnO thin film prepared from 2-methoxyethanol (Fig. 2b) exhibits a uniform and well-defined morphology. The measured thickness values are 129.5 nm and 129.6 nm, indicating minimal variation across the cross-section. The higher boiling point of 2-methoxyethanol (≈124 °C) allows for slower evaporation, promoting controlled deposition and efficient relaxation of mechanical stresses. Consequently, the film consists of clearly defined and uniformly distributed nanoparticles, consistent with its homogeneous thickness [30–32].

In addition to SEM analysis, the topographical properties of the ZnO thin films were investigated using atomic force microscopy (AFM). Figs. 2c and 2d show 2D AFM images of selected areas of the ZnO thin films, scanned over a 10 μm × 10 μm area, with corresponding 3D AFM micrographs of the same samples shown in the insets, illustrating the spatial distribution of surface roughness. For ZnO thin films prepared from methanol, a pronounced mountain-like, wrinkled surface structure is clearly visible (Fig. 2c). This morphology is consistent with the previously discussed effects of rapid methanol evaporation and the resulting mechanical stresses during drying. In contrast, ZnO thin films synthesized using 2-methoxyethanol (Fig. 2d) exhibit a significantly more homogeneous and uniform surface structure, in full agreement with the SEM results. Additionally, the surface roughness of ZnO thin films is significantly higher for films prepared from methanol (21 nm rms) compared to those prepared using 2-methoxyethanol (2.8 nm rms).

3.2. Optical properties

The optical properties of ZnO thin films were investigated by diffuse reflectance spectroscopy (DRS) in the UV–visible range. Since the films do not have an ideally smooth surface, specular reflection is not applicable, and DRS allows the analysis of light scattering from the surface and the determination of key optical parameters. The UV–Vis DRS spectra (Fig. 3) show characteristic reflection curves for ZnO films obtained from solutions with methanol and 2-methoxyethanol, in both cases exhibiting a sharp rise in reflection around 370 nm, which corresponds to the direct band gap of ZnO.

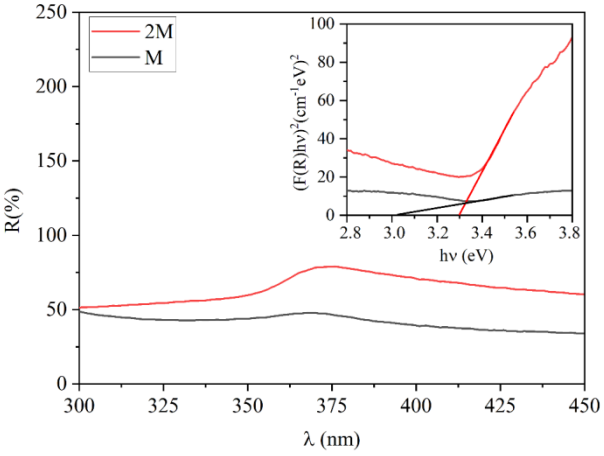

Figure 3. UV–Vis diffuse reflectance spectra (DRS) of ZnO thin films prepared from methanol- and 2-methoxyethanol-based solutions, with the Kubelka-Munk plots for the band gap energy determination shown in the inset

For the quantitative determination of the band gap width, the Kubelka–Munk model was applied, which enables the correlation between light absorption and reflection for irregular surfaces.

$$F(R) = \frac{(1-R)^2}{2R} \qquad (6)$$

The measured values of R (%) were converted into $F(R)$, and then, for the determination of the band gap width, a plot of $[F(R) \times E]^2$ as a function of E (eV) was constructed (inset of Fig. 3). The band gap width was determined by extrapolating the linear portion of the $[F(R) \times E]^2$ curve with respect to E (eV) to zero. As previously established, the band gap width depends on the crystallite size. For ZnO films prepared with methanol as the solvent, it is around 3 eV, which is lower compared to films prepared with 2-

methoxyethanol, where it is approximately 3.3 eV. In both cases, it is lower than the value of 3.37 eV reported for bulk ZnO. This red shift of the band gap energy is a consequence of the agglomeration of nanocrystals into larger crystallites, as reported by various authors in the literature [33,34].

As mentioned earlier, films prepared from 2-methoxyethanol exhibit a more homogeneous distribution of nanoparticles and a more uniform surface, which allows for more stable and predictable light absorption. In contrast, the wrinkled surface of films prepared with methanol results in higher roughness and local light scattering. In this way, the connection between the morphological characteristics and the optical performance of ZnO thin films is clearly evident.

4. CONCLUSIONS

Thin-layered ZnO films were successfully fabricated using the spin-coating technique with methanol and 2-methoxyethanol on p-type Si (100) substrates. Microstructural analysis by XRD, using the Williamson–Hall method, showed that the crystallite sizes are larger than the values obtained from the Debye–Scherrer method, indicating the significant role of strain in peak broadening. Deformation parameters, stress, and energy density, determined using the UDM, USDM, and UDEDM models, were higher for films prepared with 2-methoxyethanol compared to methanol, suggesting increased internal stability and homogeneity of these films. Morphological analysis by SEM and AFM revealed that ZnO films prepared with 2-methoxy ethanol are significantly more homogeneous, with low roughness, whereas films from methanol exhibit pronounced surface wrinkling. Optical characterization using UV–Vis DRS and application of the Kubelka–Munk theory showed that films prepared with 2-methoxyethanol have a slightly wider band gap (≈3.3 eV) compared to methanol-based films (≈3.02 eV), both being lower than that of bulk ZnO (≈3.37 eV).

Thus, the choice of solvents (fabrication conditions) strongly influence the microstructure, morphology, and optical properties of ZnO thin films. Films prepared with 2-methoxyethanol, due to their higher homogeneity, more stable internal stresses, and favorable optical characteristics, represent excellent candidates for a variety of applications.

Acknowledgements

This work was supported by the Federal Ministry of Science and Education of the Bosnia and Herzegovina (No. 01-3840-VI-1/23). We would like to thank Kerim Hrvat for his assistance during XRD measurements in Sarajevo and Jelena Potočnik for the cross-section SEM micrographs in Belgrade.

5. REFERENCES

[1] E. K. Richman, J. E. Hutchison. (2009). The nanomaterial characterization bottleneck. ACS Nano, 3(9), 2441–2446. https://doi.org/10.1021/nn901112p

[2] S. Napolitano, E. Glynos, N. B. Tito. (2017). Glass transition of polymers in bulk, confined geometries, and near interfaces. Reports on Progress in Physics, 80(3), 036602. https://doi.org/10.1088/1361-6633/aa5284

[3] A. P. Alivisatos. (1996). Semiconductor clusters, nanocrystals, and quantum dots. Science, 271(5251), 933–937. https://doi.org/10.1126/science.271.5251.933

[4] D. C. Look. (2001). Recent advances in ZnO materials and devices. Materials Science and Engineering: B, 80(1-3), 383–387. https://doi.org/10.1016/S0921-5107(00)00604-8

[5] T. Minami. (2005). Transparent conducting oxide semiconductors for transparent electrodes. Semiconductor Science and Technology, 20(4), S35–S44. https://doi.org/10.1088/0268-1242/20/4/004

[6] L. Spanhel, M. A. Anderson. (1991). Semiconductor clusters in the sol-gel process: Quantized aggregation, gelation, and crystal growth in concentrated zinc oxide colloids. Journal of the American Chemical Society, 113(8), 2826–2833. https://doi.org/10.1021/ja00008a004

[7] S. O'Brien, L. H. K. Koh, G. M. Crean. (2008). ZnO thin films prepared by a single step sol-gel process. Thin Solid Films, 516, 1391–1395. https://doi.org/10.1016/j.tsf.2007.03.160

[8] M. Ohyama, H. Kozuka, T. Yoko, S. Sakka. (1996). Preparation of ZnO films with preferential orientation by sol-gel method. Journal of the Ceramic Society of Japan, 104(4), 296–300. https://doi.org/10.2109/jcersj.104.296

[9] K. Matsubara, P. Fons, K. Iwata, A. Yamada, K. Sakurai, H. Tampo, S. Niki. (2003). ZnO transparent conducting films deposited by pulsed laser deposition for solar cell applications. Thin Solid Films, 431–432, 369–372. https://doi.org/10.1016/S0040-6090(03)00243-8

[10] C. M. Oral, M. Ussia, M. Pumera. (2022). Hybrid enzymatic/photocatalytic degradation of antibiotics via morphologically programmable light-driven ZnO microrobots. Small, 18(39), 2202600. https://doi.org/10.1002/smll.202202600

[11] S. Jadoun, J. Yáñez, H. D. Mansilla, U. Riaz, N. P. S. Chauhan. (2022). Conducting polymers/zinc oxide-based photocatalysts for environmental remediation: A review. Environmental Chemistry Letters, 20(3), 2063–2083. https://doi.org/10.1007/s10311-022-01398-w

[12] G. Gadacz, S. Beaudet-Savignat, L. Longuet, J.-L. Longuet. (2013). Influence of the preparation

process on the electrical properties of high-field co-doped zinc oxide varistors. Ceramics International, 39(8), 8869–8875. https://doi.org/10.1016/j.ceramint.2013.04.080

[13] P. Rong, S. Ren, Q. Yu. (2018). Fabrications and applications of ZnO nanomaterials in flexible functional devices — a review. Critical Reviews in Analytical Chemistry, 49(4), 336–349. https://doi.org/10.1080/10408347.2018.1531691

[14] F. Tabataba-Vakili, C. Brimont, B. Alloing, B. Damilano, L. Doyennette, T. Guillet, M. El Kurdi, S. Chenot, V. Brändli, E. Frayssinet, J.-Y. Duboz, F. Semond, B. Gayral, P. Boucaud. (2020). Applied Physics Letters, 117, 121103. https://doi.org/10.1063/5.0015252

[15] S. K. Arya, S. Saha, J. E. Ramirez-Vick, V. Gupta, S. Bhansali, S. P. Singh. (2012). Recent advances in ZnO nanostructures and thin films for biosensor applications: Review. Analytica Chimica Acta, 737, 1–21. https://doi.org/10.1016/j.aca.2012.05.048

[16] D. Coutancier, S.-T. Zhang, S. Bernardini, O. Fournier, T. Mathieu-Pennober, F. Donsanti, M. Tchernycheva, M. Foldyna, N. Schneider. (2020). ALD of ZnO:Ti: Growth mechanism and application as an efficient transparent conductive oxide in silicon nanowire solar cells. ACS Applied Materials & Interfaces, 12, 21036–21044. https://doi.org/10.1021/acsami.9b22973

[17] T. Minami, H. Nanto, S. Takata. (1985). Highly conductive and transparent ZnO thin films prepared by r.f. magnetron sputtering in an applied external d.c. magnetic field. Thin Solid Films, 124(1), 43–47. https://doi.org/10.1016/0040-6090(85)90026-4

[18] B. S. Li, Y. C. Liu, Z. S. Chu, D. Z. Shen, Y. M. Lu, J. Y. Zhang, X. W. Fan. (2002). High quality ZnO thin films grown by plasma enhanced chemical vapor deposition. Journal of Applied Physics, 91(1), 501–505. https://doi.org/10.1063/1.1415545

[19] W. S. Hu, Z. G. Liu, X. L. Guo, C. Lin, S. N. Zhu, D. Feng. (1995). Preparation of c-axis oriented ZnO optical waveguiding films on fused silica by pulsed laser reactive ablation. Materials Letters, 25, 5–8.

[20] L. J. Mandalapu, F. X. Xiu, Z. Yang, J. L. Liu. (2006). Mater. Res. Soc. Symp. Proc., 891, 351.

[21] J. L. Yang, S. J. An, W. I. Park, G. C. Yi, & W. Choi. (2004). Photocatalysis using ZnO thin films and nanoneedles grown by metal-organic chemical vapor deposition. Advanced Materials, 16(18), 1661–1664. https://doi.org/10.1002/adma.200306673

[22] A. Aashour, M. A. Kaid, N. Z. El-Sayed, A. A. Ibrahim. (2006). Physical properties of ZnO thin films deposited by spray pyrolysis technique. Applied Surface Science, 252(22), 7844–7848. https://doi.org/10.1016/j.apsusc.2006.03.062

[23] D. Chen. (2001). Anti-reflection (AR) coatings made by sol–gel processes: A review. Solar Energy Materials and Solar Cells, 68(3–4), 313–336. https://doi.org/10.1016/S0927-0248(00)00136-0

[24] N. Sahu, B. Parija, S. Panigrahi. (2009). Fundamental understanding and modeling of spin coating process: A review. Indian Journal of Physics, 83, 319–324. https://doi.org/10.1007/s12648-009-0009-z

[25] M. Purica, E. Budianu, E. Rusu. (2000). Heterojunction with ZnO polycrystalline thin films for optoelectronic devices applications. Microelectronic Engineering, 51–52, 425–431. https://doi.org/10.1016/S0167-9317(00)00248-0

[26] M. H. Huang, Y. Wu, H. Feick, N. Tran, E. Weber, P. Yang. (2001). Catalytic growth of zinc oxide nanowires by vapor transport. Advanced Materials, 13(2), 113–116. https://doi.org/10.1002/1521-4095(200101)13:2

[27] M. Kashif, S. M. Usman Ali, M. E. Ali, H. I. Abdulgafour, U. Hashim, M. Willander, Z. Hassan. (2012). Morphological, optical, and Raman characteristics of ZnO nanoflakes prepared via a sol–gel method. Physica Status Solidi (A), 209(1), 143–147. https://doi.org/10.1002/pssa.201127501

[28] S. Fatimah, R. Ragadhita, D. F. Al Husaeni, A. B. D. Nandiyanto. (2022). How to calculate crystallite size from X-ray diffraction (XRD) using Scherrer method. ASEAN Journal of Science and Engineering, 2(1), 65–76. https://doi.org/10.17509/ajse.v2i1.37647

[29] D. Nath, F. Singh, R. Das. (2020). X-ray diffraction analysis by Williamson-Hall, Halder-Wagner and size-strain plot methods of CdSe nanoparticles—a comparative study. Materials Chemistry and Physics, 239, 122021. https://doi.org/10.1016/j.matchemphys.2019.122021

[30] A. Modrić-Šahbazović, Z. Sakić, M. Đekić, S. Isaković, I. Gazdić. (2025). The influence of solvent and number of layers on the homogeneity and properties of ZnO thin films obtained by spin-coating method. Processing and Application of Ceramics, 19(2), 150–156. https://doi.org/10.2298/PAC2502150M

[31] D. Guo, Y. Ju, C. Fu, Z. Huang, L. Zhang. (2016). (002)-oriented growth and morphologies of ZnO thin films prepared by sol-gel method. Materials Science-Poland, 34, 555–563. https://doi.org/10.1515/msp-2016-0076

[32] K. L. Foo, U. Hashim, K. Muhammad, C. H. Voon. (2014). Sol–gel synthesized zinc oxide nanorods and their structural and optical investigation for optoelectronic application. Nanoscale Research Letters, 9(1), 429. https://doi.org/10.1186/1556-276X-9-429

[33] H. L. Hartnagel, A. L. Dawar, A. K. Jain, C. Jagadish. (1995). Semiconducting transparent thin films. Bristol, UK: Institute of Physics Publishing.

[34] J. I. Pankove. (1975). Optical progress in semiconductors. New York, NY: Dover.

IZVOD

OPTIMIZACIJA MIKROSTRUKTURNIH I OPTIČKIH SVOJSTAVA TANKIH ZnO FILMOVA NA P-TIPU Si(100)

Vrlo tanki ZnO filmovi su naneseni na p-tip Si(100) supstrate korištenjem dva različita rastvarača, metanol (M) i 2-metoksietanol (2M), jednostavnom spin-coating metodom. Petoslojni ZnO filmovi su strukturno karakterizovani pomoću rendgenske difrakcije (XRD), pri čemu je detaljna analiza izvršena primjenom Williamson–Hall (W–H) metode. Površinska morfologija ispitana je skenirajućom elektronskom mikroskopijom (SEM) i mikroskopijom atomskih sila (AFM), dok su optička svojstva određena UV–Vis spektroskopijom, uključujući širinu zabranjene zone izračunatu prema Kubelka–Munk teoriji. Veličine kristalita izračunate W–H modelima bile su veće od onih procijenjenih Debye–Scherrer metodom, što ukazuje da je proširenje difrakcionih pikova pod uticajem i veličine kristalita i naprezanja u kristalnoj rešetki. Vrijednosti deformacije (strain), napona (stress) i gustine energije deformacije, dobijene primjenom modela uniformne deformacije (UDM), modela uniformne naponske deformacije (USDM) i modela uniformne gustine energije deformacije (UDEDM), bile su veće u filmovima pripremljenim s 2-metoksietanolom nego s metanolom. ZnO filmovi dobijeni iz 2-metoksietanola pokazali su veću homogenost i manju hrapavost površine, dok je njihova širina zabranjene zone (~3,3 eV) bila nešto veća u odnosu na filmove pripremljene s metanolom (~3,02 eV), ali i dalje manja od vrijednosti za masivni (bulk) ZnO (3,37 eV). Ovi rezultati pokazuju da tanki ZnO filmovi pripremljeni s 2-metoksietanolom imaju superiorna mikrostrukturna, mehanička i optička svojstva, formirajući glađe i ujednačenije filmove s poboljšanim optičkim karakteristikama, te se stoga češće koriste za optoelektronske i fotonaponske primjene zbog poboljšane kristaličnosti, male hrapavosti površine i odgovarajuće širine zabranjene zone.

Ključne riječi: *ZnO, tanki film, sol-gel, spin-coater, rastvarač*

Naučni rad
Rad primljen: 04.02.2026.
Rad korigovan: 24.02.2026.
Rad prihvaćen: 03.03.2026.

Almedina Modrić-Šahbazović *https://orcid.org/0009-0003-3682-3973*
Zerina Sakić *https://orcid.org/0009-0002-1389-478X*
Maja Đekić *https://orcid.org/0000-0002-5391-1268*